

# Evaluation of a risk-based environmental hot spot delineation algorithm

Parikhit Sinha<sup>\*</sup>, Michael B. Lambert, William A. Schew

*O'Brien and Gere, 512 Township Line Road, Two Valley Square, Suite 120, Blue Bell, PA 19422, USA*

Received 25 April 2006; received in revised form 10 August 2006; accepted 31 March 2007

Available online 6 April 2007

## Abstract

Following remedial investigations of hazardous waste sites, remedial strategies may be developed that target the removal of “hot spots,” localized areas of elevated contamination. For a given exposure area, a hot spot may be defined as a sub-area that causes risks for the whole exposure area to be unacceptable. The converse of this statement may also apply: when a hot spot is removed from within an exposure area, risks for the exposure area may drop below unacceptable thresholds. The latter is the motivation for a risk-based approach to hot spot delineation, which was evaluated using Monte Carlo simulation. Random samples taken from a virtual site (“true site”) were used to create an interpolated site. The latter was gridded and concentrations from the center of each grid box were used to calculate 95% upper confidence limits on the mean site contaminant concentration and corresponding hazard quotients for a potential receptor. Grid cells with the highest concentrations were removed and hazard quotients were recalculated until the site hazard quotient dropped below the threshold of 1. The grid cells removed in this way define the spatial extent of the hot spot. For each of the 100,000 Monte Carlo iterations, the delineated hot spot was compared to the hot spot in the “true site.” On average, the algorithm was able to delineate hot spots that were collocated with and equal to or greater in size than the “true hot spot.” When delineated hot spots were mapped onto the “true site,” setting contaminant concentrations in the mapped area to zero, the hazard quotients for these “remediated true sites” were on average within 5% of the acceptable threshold of 1.

© 2007 Elsevier B.V. All rights reserved.

*Keywords:* Hazardous waste; Site remediation; Geospatial analysis; Risk assessment

## 1. Introduction

Following remedial investigations of hazardous waste sites, remedial strategies may be developed that target the removal of “hot spots,” localized areas of elevated contamination. Hot spot remediation is important to hazardous site cleanup because it focuses remedial efforts on smaller targeted areas and reduces the potential future mass flux of contaminants from these areas. Hot spot delineation falls under the broader category of spatial data analysis for which a variety of methods have been proposed [1]. Kulldorff [2] proposed the spatial scan statistic for identifying hot spots by determining the probability that a given spatial response cluster could occur by chance variation. Other past approaches to hot spot delineation include sweep-out methods in which available measurements are used to form best linear unbiased predictions for unquantified areas [3]. Maximum entropy methods have also been used in conjunction with

pre-defined hot spot thresholds to determine the probability that components of composite samples exceed hot spot thresholds when the composite itself does not [4].

A risk-based approach to hot spot delineation may also be used to guide site characterization and remedial strategy. For a given exposure area, a hot spot may be defined as a sub-area that causes risks for the whole exposure area to be unacceptable [5]. The converse of this statement may also apply: when a hot spot is removed from within an exposure area, risks for the exposure area drop below unacceptable thresholds. The latter is the motivation for a risk-based approach to hot spot delineation.

An example of such an approach follows. Suppose a former chemical storage site has been selected for remediation, with the goal of converting the property into a park for public use. Several rounds of field sampling have been performed to characterize the nature and extent of contamination at the site. Exposure scenarios have been developed and health risks to potential current and future human receptors have been evaluated. Based on the 95% upper confidence limit (UCL) of mean contaminant concentrations at the site and an exposure scenario for a future child recreational visitor to the site, an unacceptable rea-

<sup>\*</sup> Corresponding author. Tel.: +1 215 628 9107x245; fax: +1 215 628 9953.  
E-mail address: [sinhap@obg.com](mailto:sinhap@obg.com) (P. Sinha).

sonable maximum exposure (RME) hazard quotient ( $HQ \geq 1$ ) is estimated for incidental ingestion of a contaminant (e.g., antimony) in surface soil by the child recreator. For the purpose of this example and subsequent experimental methods, other potential exposure pathways (e.g., dermal contact and inhalation) are minor compared to the ingestion pathway and are not considered.

Closer examination of the antimony samples reveals that the 95% UCL is influenced by a few high samples, which raise the mean, variance, and, therefore, the 95% UCL of the antimony concentrations. Furthermore, removal of only the top 5 detected samples would lower the UCL to a concentration low enough to lead to an acceptable  $HQ (<1)$ . A sub-area within the exposure area, which contains the top 5 detected samples, could be delineated as a hot spot, since removal of this sub-area lowers risk in the exposure area to acceptable levels.

The value of such a delineation is two-fold: to focus the remedial effort on a targeted region, and to quantify the effect of such remediation on site risks to human health. Implementation of such a risk-based approach to hot spot delineation has been assisted by the development of geospatial statistical tools such as the Spatial Analysis and Decision Assistance (SADA; [6]) model developed by the University of Tennessee and Oak Ridge National Laboratory. However, the effectiveness of risk-based hot spot delineation methods has not been quantitatively evaluated. In addition, hot spot delineation methods may have spatial bias due to the uneven spacing of environmental samples.

The purpose of this study is to quantitatively evaluate a risk-based, spatially unbiased approach to hot spot delineation. The procedure is evaluated by assessing risk reductions in a virtual contaminated site following removal of delineated hot spots. Monte Carlo simulation is used to evaluate the procedure for a variety of sample data sets, where both the number and location of samples is allowed to vary randomly.

The hot spot delineation algorithm evaluated here is an alternative to the traditional approach of using regulatory screening levels (e.g., soil screening levels) to determine site cleanup goals. For example, if an entire exposure area is remediated down to a soil screening level and the risks are then recalculated for that exposure area, the risks will be significantly lower than acceptable thresholds. In other words, the use of soil screening levels leads to an “over-cleaning” of the site, because it is not required that the entire exposure area be below the soil screening level, only that the 95% UCL of the mean constituent concentration for the exposure area be below the soil screening level. Therefore, some site concentrations can exceed the soil screening level without the site as a whole having unacceptable risks. Furthermore, soil screening levels are based on a single exposure scenario (e.g., residential), whereas the hot spot delineation algorithm evaluated here can accommodate any specified exposure scenario.

## 2. Methods

The risk-based hot spot delineation algorithm was designed to simulate field sampling and data analysis procedures conducted during actual remedial investigations. In environmental

sampling, two main parameters are under the investigator’s control: the number and location of samples. Consequently, these were the main parameters varied in the Monte Carlo simulation.

Specifically, a virtual site (100 ft  $\times$  100 ft; Fig. 1a) with a continuous contaminant distribution was generated using an arbitrary analytical function of form  $z=f(x, y)$  with a single maximum at  $x=10, y=10$ :

$$C_s = 0.4 \times [(50 - \text{abs}(x - 10))] \times [(50 - \text{abs}(y - 10))] \quad (1)$$

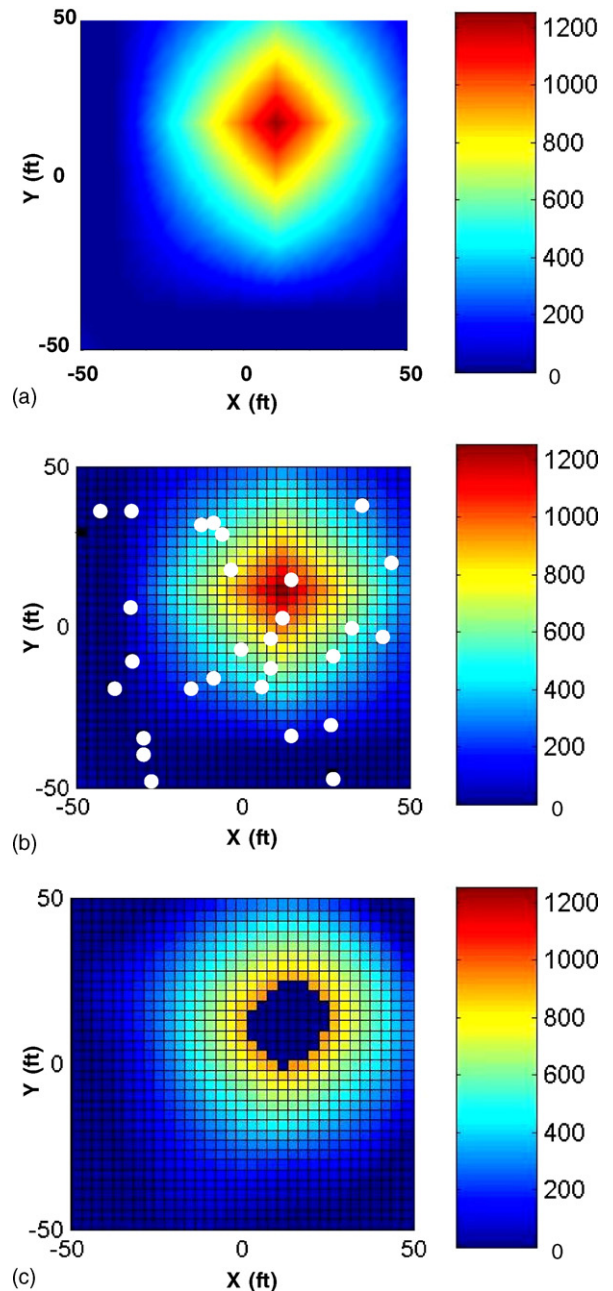


Fig. 1. Antimony concentration (mg/kg) in surface soil in (a) the true site, (b) the interpolated site for one iteration of the Monte Carlo simulation, and (c) the interpolated site in (b) with hot spot delineated. The locations of random samples drawn from (a) to create the interpolated site for this Monte Carlo iteration are shown in (b) as white circles.

where  $C_s$  is the contaminant concentration in surface soil (mg/kg),  $x$  and  $y$  are site coordinates (in ft), and  $\text{abs}$  is the absolute value of the term. A random number of samples were drawn from random locations in this virtual site, which will be referred to as the “true site.” The random spacing of the sample data reflects the common practical case where data sets collected over time do not follow a single uniform grid spacing. The random samples drawn from a parent distribution reflects the practical case of taking a finite number of field samples to try to characterize a parent contaminant population.

The sample data set is the starting point of the risk-based hot spot delineation procedure. The samples were assigned to a blank (100 ft  $\times$  100 ft) grid with 5 ft  $\times$  5 ft grid boxes. The samples were used to generate a site contaminant distribution by interpolating between sample points using biharmonic spline, a commercially available (Matlab V. 11) interpolation algorithm. The biharmonic spline finds the minimum curvature surface that passes through a set of non-uniformly spaced data points using a linear combination of Green functions centered at each data point [7].

This interpolation method was chosen on the basis of inter-comparisons between the interpolated concentrations and the true site concentrations. The site resulting from interpolation of the sample data set will be referred to as the “interpolated site.” Fig. 1b shows an interpolated site corresponding to a sample data set of 28 samples randomly drawn from the virtual site in Fig. 1a. The locations of the sample data are shown with white circles in Fig. 1b. The average concentration in each of the 400 grid cells of the interpolated site was tabulated to create an “interpolated data set” of 400 samples (1 for each grid cell). The interpolated data set was used to calculate the 95% UCL of the mean site contaminant concentration using the non-parametric Chebyshev theorem:

$$\text{UCL} = x + \left( \frac{s}{\sqrt{\alpha \times n}} \right) \quad (2)$$

where  $x$  is the mean,  $s$  is the standard deviation,  $\alpha$  is 0.05 (1 – confidence limit), and  $n$  is the sample size.

By using the interpolated data set to determine the 95% UCL, there was no spatial bias in the UCL calculation since the data points in the interpolated data set are uniformly spaced. This is in contrast to the sample data drawn from the true site, which are not uniformly spaced. Since the purpose of the 95% UCL is to provide an upper-bound estimate of concentrations over the entire exposure area, it is important that the data used to calculate the UCL is spaced uniformly over the exposure area.

A hazard quotient (HQ) for incidental ingestion of a contaminant (antimony in surface soil) by a recreational child (age <6 years) was calculated using the following equation [8]:

$$\text{HQ} = \frac{\text{EPC} \times \text{CF} \times \text{IR} \times \text{FI} \times \text{EF} \times \text{ED}}{\text{BW} \times \text{AT} \times \text{RfD}} \quad (3)$$

where EPC (exposure point concentration) is the 95% UCL for antimony in surface soil in the interpolated data set (mg/kg), CF (conversion factor) is  $1 \times 10^{-6}$  kg/mg, IR (surface soil incidental ingestion rate) is 200 mg/day, FI (fraction ingested) is 1, EF (exposure frequency) is 44 days/year, ED (exposure duration) is

6 years, BW (body weight) is 15 kg, AT (averaging time) = 2190 days, and RfD (oral reference dose for antimony for non-cancer toxicity) is 0.004 mg/(kg  $\times$  day). The exposure factors and the toxicity reference dose above were obtained from USEPA [9] and USEPA [10], respectively. The use of the 95% UCL as the EPC and the conservative exposure factors selected are consistent with a reasonable maximum exposure (i.e., conservative) estimation of risk [8].

For an overall site  $\text{HQ} \geq 1$ , the individual grid cell in the interpolated site with the highest contaminant concentration was removed (concentration set to 0). Following the removal, the 95% UCL and the corresponding site HQ were recalculated. This process of preferentially removing those cells with the highest contaminant concentrations and recalculating the site HQ was repeated until the site HQ dropped below 1. The grid cells removed in this way define the spatial extent of the hot spot delineation, since removal of the cells lowers the site HQ to < 1. Fig. 1c shows the delineated hot spot for the interpolated site in Fig. 1b.

The above process was repeated in a Monte Carlo simulation of 100,000 iterations in which the virtual true site was kept constant, but both the number (15–100) and spacing of samples drawn from the true site were allowed to vary randomly. In practice, the number of samples to take and their locations are fundamental decisions made in field investigations to help characterize the extent of contamination. By allowing these terms to vary, we can evaluate their effect on the hot spot delineation algorithm. The range of sample sizes (15–100) was arbitrarily selected but allows the hot spot delineation algorithm to be evaluated for both sparsely sampled and densely sampled sites. The sample size was drawn from a uniform distribution between 15 and 100 so that each value had an equal chance of being drawn over the course of the 100,000 Monte Carlo iterations.

To quantify the results of the Monte Carlo simulation, the extent and location of the estimated hot spot were compared to that of the “true hot spot.” The latter was determined by applying the above hot spot algorithm to the true site (for which all the site concentrations are known) to determine what area would have to be removed to lower the true site HQ (for ingestion of antimony by a child recreator) to <1. The extent of this true hot spot is 599 ft<sup>2</sup>, centered around coordinates ( $x=9.95$  ft,  $y=10.00$  ft). The center was determined by averaging the  $x$  and  $y$  coordinates of all the grid cells within the true hot spot area. For each Monte Carlo iteration, the extent and center of the predicted hot spot was compared to the above “true” values.

Although the hot spot delineation algorithm was evaluated for a specific and arbitrary exposure scenario (ingestion of antimony), it can be used for other cases as long as sample concentrations, an exposure route, and a risk standard (e.g., hazard quotient, cancer risk) are available. Even for more complex transport processes such as migration of soil to groundwater, risk standards for exposure to groundwater exist, and migration of soil to groundwater can be modeled from soil concentrations as part of a given exposure route; therefore, the hot spot delineation algorithm can be applied.

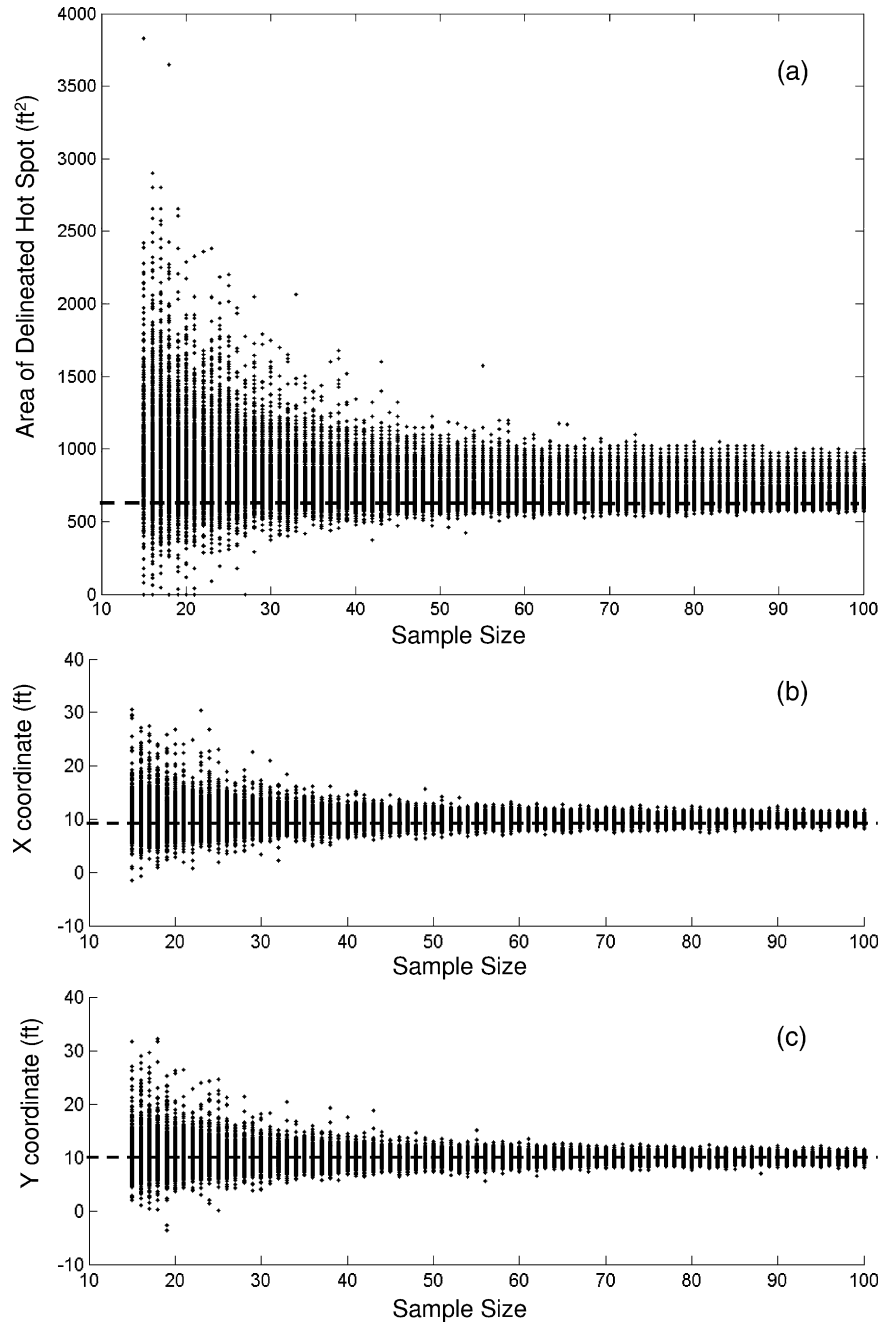


Fig. 2. (a) Area extent (ft<sup>2</sup>) of delineated hot spots versus sample size, (b) X coordinate (ft) of center of delineated hot spots vs. sample size, and (c) Y coordinate (ft) of center of delineated hot spots vs. sample size for a Monte Carlo simulation of 100,000 iterations. Dashed line in (a) indicates the area extent of the true hot spot. Dashed lines in (b) and (c) indicate X and Y coordinates, respectively, of the center of the true hot spot.

### 3. Results

The area extent of predicted hot spots as a function of number of samples is shown in Fig. 2a for a Monte Carlo simulation of 100,000 iterations. The average ( $\mu$ ) predicted hot spot area is 811 ft<sup>2</sup>, with a standard deviation ( $\sigma$ ) of 143 ft<sup>2</sup>. The variance of the estimated hot spot area is highest for lower sample sizes ( $n < 40$ ,  $\sigma = 203$  ft<sup>2</sup>), as the likelihood that samples will be randomly drawn from within the true hot spot decreases for low sample sizes, resulting in a wide range of predicted hot spots. As the sample density increases ( $n \geq 40$ ), the magnitude

of the predicted hot spot area converges ( $\mu = 787$  ft<sup>2</sup>,  $\sigma = 101$  ft<sup>2</sup>). This value still exceeds the true hot spot area (599 ft<sup>2</sup>), and for the entire simulation, the estimated hot spot area exceeds the true hot spot area in 97% of cases. This is largely due to the use of the Chebyshev theorem (Eq. (2)) in calculating site 95% UCLs, which is a conservative approach that leads to an overestimate of the site hazard quotient, forcing a larger area to be removed to lower the site HQ to 1. The Chebyshev theorem was used because it is a non-parametric method and can, therefore, be applied to any sample distribution. However, a distribution-specific method (e.g., t-statistic for normally distributed data)

may be used in place of the Chebyshev theorem when the sample distribution is known. In sum, the Monte Carlo simulation provides  $\sim 97\%$  confidence that the predicted hot spot is at least as large as the true hot spot. Conservative overestimation of the hot spot area during remedial design is favorable because it increases the likelihood of remedial effectiveness, thus lowering risk.

However, even if the spatial extent of the predicted hot spot is sufficient, it must be located properly within the site. Fig. 2b and c shows the coordinates of the predicted hot spot center as a function of the number of samples in the Monte Carlo simulation. The coordinates were obtained by averaging the  $x$  and  $y$  coordinates of all the grid cells within a predicted hot spot. On average, the coordinates of the center of the predicted hot spots are  $x = 10.08$  ft ( $\sigma_x = 1.16$  ft) and  $y = 10.08$  ft ( $\sigma_y = 1.15$  ft). These average predicted coordinates are within a standard deviation of the center of the true hot spot ( $x = 9.95$  ft,  $y = 10.00$  ft). As with Fig. 2a, the variance in Fig. 2b and c decreases as the sample size increases ( $\sigma_x = \sigma_y = 1.87$  for  $n < 40$ ;  $\sigma_x = \sigma_y = 0.66$  for  $n \geq 40$ ). With increasing sample size, the likelihood of randomly sampling within the true hot spot increases, resulting in more consistency in the estimated hot spot location. For  $n \geq 40$ , the average coordinates of the predicted hot spot center converge to  $x = 10.00$  ft and  $y = 10.00$  ft, nearly equal to the true hot spot center coordinates.

Based on the results of this Monte Carlo simulation, the hot spots predicted in the simulation are, on average, collocated with and at least as large as the true hot spot. However, in order to meet the definition of a hot spot, the delineated area (when removed) must result in reduction of the site  $HQ < 1$ . Therefore, in order to verify the hot spot delineation algorithm, the predicted hot spot in a Monte Carlo iteration was mapped onto the true site,

setting contaminant concentrations to zero within the mapped area. The resulting site may be referred to as the “remediated true site.” The average contaminant concentration in each grid cell of the remediated true site was tabulated and used to calculate the 95% UCL (Eq. (2)) and site HQ (Eq. (3)). For  $HQ < 1$  in the remediated true site, the hot spot delineation algorithm may be deemed successful.

Fig. 3 shows the HQ of the remediated true site as a function of sample size in the Monte Carlo simulation. On average, the HQ is 1.03 ( $\sigma = 0.03$ ), slightly above the desired threshold of 1. The variance of the HQ decreases for larger sample size ( $\sigma = 0.05$  for  $n < 40$ ;  $\sigma = 0.01$  for  $n \geq 40$ ), as the hot spot algorithm is able to perform more consistently with greater sample density. For  $n \geq 40$ , the remediated true site also has an average HQ of 1.03, within 5% of the acceptable threshold ( $HQ = 1$ ).

In order for the HQ of the remediated true site to be  $\leq 1$ , the center of the delineated hot spot has to be collocated with the center of the true hot spot and the area of the delineated hot spot has to be at least as large as the area of the true hot spot. While these conditions are met on average (Fig. 2) in the Monte Carlo simulation, for an individual iteration of the simulation, the conditions are not exactly met, resulting in numerous iterations where the remediated true site has  $HQ > 1$  (Fig. 3). Nevertheless, the remediated site HQ's are largely  $< 1.1$ , which represents manageable and acceptable risk from a risk management perspective.

#### 4. Discussion

Based on a Monte Carlo simulation of 100,000 iterations, delineated hot spots are, on average, collocated with and equal to or greater in size than the “true hot spot.” However, a num-

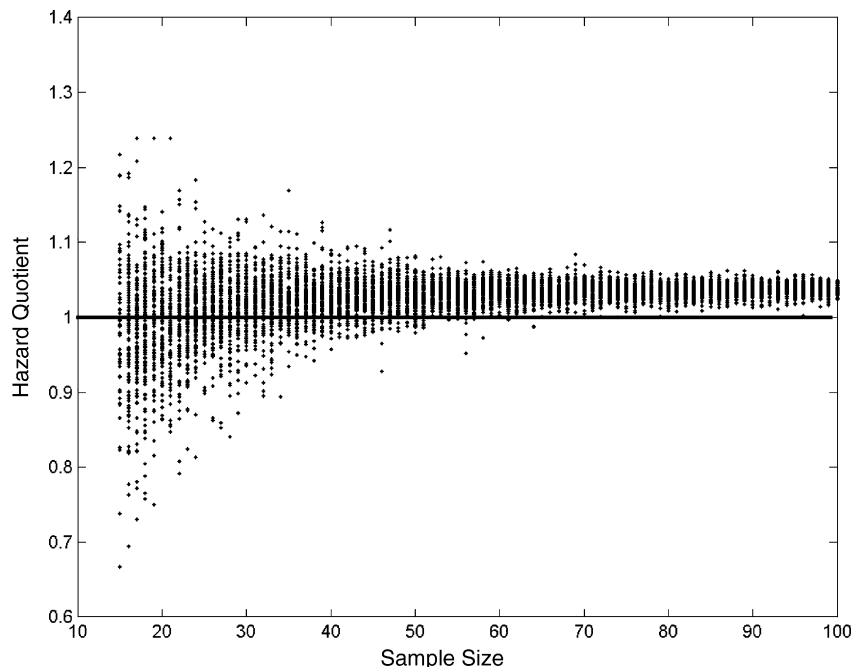


Fig. 3. Hazard quotients of the remediated true sites versus sample size for a Monte Carlo simulation of 100,000 iterations. Dashed line indicates the hazard quotient threshold for acceptable risk.

ber of factors influence the delineation process, as discussed below.

#### 4.1. Interpolation

The choice of interpolation method will affect the hot spot delineation algorithm by affecting the contaminant concentrations in the interpolated site. Common interpolation methods include linear, polynomial, kriging, inverse distance weighted, etc. The differences between interpolation methods become particularly exaggerated when samples are sparse. However, as will be discussed below (Section 4.3), confidence in the delineation algorithm is generally low for low sample density, making the choice of interpolation method less critical.

The interpolation method used in this study (biharmonic spline) was chosen after comparing interpolated concentrations with true site concentrations and repeating over a number of iterations. Because this study used Monte Carlo simulation to evaluate a hot spot delineation algorithm, it was essential that the interpolation method chosen could be easily implemented within a Monte Carlo framework (i.e., numerous iterations with minimal processing demands). If the hot spot delineation algorithm were run for fewer iterations, as would be the case for applications to field data (see Section 4.4), other more sophisticated interpolation methods could be used. For example, universal kriging, though encumbered with large estimation uncertainties, is available for extension to unsampled locations, a condition that the biharmonic spline algorithm does not effectively handle.

#### 4.2. Multiple hot spots

Thus far, the hot spot delineation algorithm has been evaluated for a virtual site with a single, sizable ( $600 \text{ ft}^2$ ) hot spot. To extend the evaluation, additional simulations were performed for virtual sites with multiple (2–4), smaller hot spots. For example, Fig. 4a shows a virtual site with four hot spots whose respective “true areas” sum to  $400 \text{ ft}^2$ . The same exposure scenario as used in the single hot spot delineation (incidental ingestion of antimony in surface soil by a recreational child) was used for the multiple hot spot delineation. Fig. 4b shows hot spots delineated given a sample data set of 75 samples randomly drawn from the virtual site in Fig. 4a. The locations of the sample data are shown as white circles in Fig. 4a.

In general, the larger a given hot spot (relative to the total site area), the more effective the hot spot algorithm, due to the increased likelihood of randomly sampling within the hot spot. It should be noted that within a risk-based approach to hot spot delineation, the size of the total site area is not arbitrary, but rather reflects the exposure area for a potential receptor. In the case of the child recreator, the total site area might be the grounds of a park, but would not, for example, include a fenced-off area not accessible to recreators. Accurate specification of the site area is important to the hot spot algorithm because a larger site area (for a hot spot of fixed size) has lower overall site risks due to the presence of larger uncontaminated areas. Therefore, in a larger site area, a smaller hot spot would have to be removed to result in acceptable overall site risks.

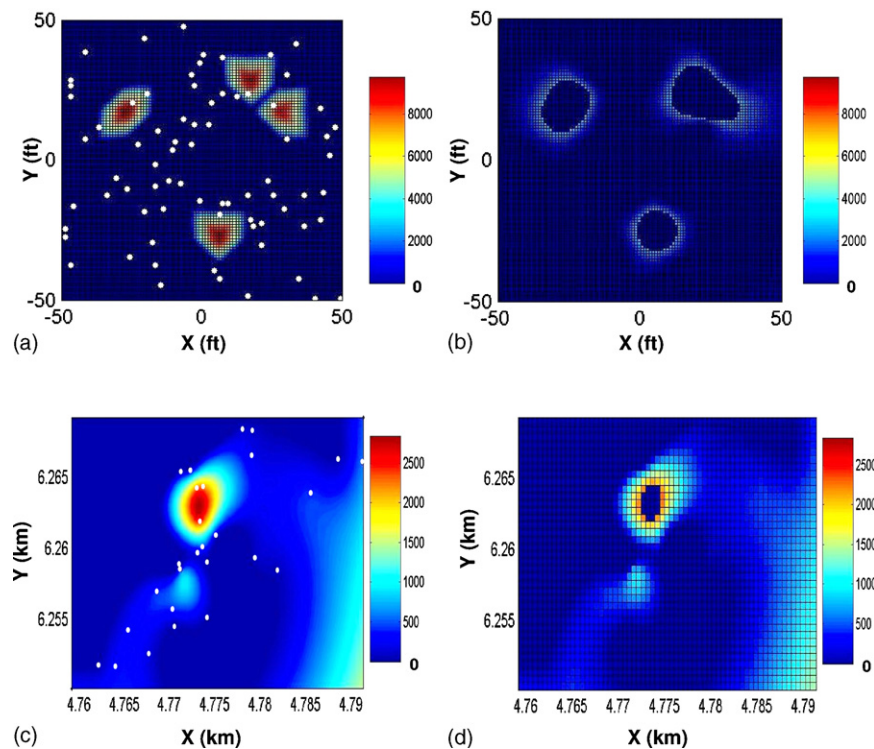


Fig. 4. Antimony concentration (mg/kg) in surface soil in (a) a true site with multiple hot spots, (b) the interpolated site corresponding to (a) with hot spot delineated, (c) an interpolated site based on field data, and (d) the interpolated site in (c) with hot spot delineated. The locations of random samples drawn from (a) to create the interpolated site in (b) are shown as white circles in (a). The locations of field samples used to create the interpolated site in (c) are shown as white circles in (c).

In addition to the relative size of the hot spot, the distance between multiple hot spots affects the hot spot algorithm. The greater the spatial separation between hot spots, the higher the likelihood of delineating distinct hot spots. In Fig. 4a, for example, the two hot spots in the northeast corner of the virtual site are too close together to be delineated as separate hot spots, given the sample density. As a result, a single hot spot is predicted for that portion of the site (Fig. 4b).

#### 4.3. Probability of not finding a hot spot

The probability of finding or not finding a given hot spot depends on the sample density relative to the hot spot dimensions. Gilbert [11] describes a Bayesian approach to hot spot sampling for a given acceptable probability of not finding a hot spot. In the case of uniformly spaced samples and a circular hot spot, the diameter of the hot spot needs to be roughly greater than or equal to the spacing between samples in order to have  $\geq 90\%$  confidence of finding the hot spot [11].

In the simulations in this study, the samples are spaced randomly, not uniformly. However, the same basic principle applies in that the ability to find a hot spot depends on the spacing between samples relative to the size of the hot spot. In Fig. 4a, for example, south of the two hot spots in the northeast corner of the site, there is a sizable area (approximately 20 ft by 30 ft) without any samples. Given no *a priori* knowledge of the site, there can be little or no confidence in being able to find a hot spot with diameter  $< 20$  ft in this location. This example highlights the importance of developing careful and strategic sampling plans, which allow for sufficient, properly spaced samples, when undertaking field investigations.

#### 4.4. Applications to field data

Thus far, the hot spot delineation algorithm has been evaluated using virtual sites for which all “true concentrations” are known. The benefit of using such sites is the ability to verify whether the algorithm succeeded in delineating the “true hot spots.” However, in practical situations, the investigator likely has minimal *a priori* knowledge of site contaminants. A historical investigation may yield information on past waste disposal practices and locations, which in turn may suggest likely hot spot locations. Such information could be used in conjunction with a Bayesian hot spot sampling approach [11] to conduct hot spot sampling with a well-defined probability of success. However, in many cases, such historical information is imprecise or not available.

Fig. 4c and d shows the results of applying the hot spot algorithm to a field data set, once again, for antimony in surface soil with respect to incidental ingestion by a child recreator. In this example, of course, there is no “true site” that is known ahead of time. The only data available is a sample data set of 27 samples shown as white circles in Fig. 4c, which also shows the interpolated site created using the sample data. The hot spot area that was removed to reduce the hazard quotient of the interpolated site to  $< 1$  is shown in Fig. 4d.

In keeping with the discussions above, a few qualifications must be made about this delineation. Since there is no “true site” to compare to, we must exercise caution in evaluating the results of the hot spot delineation. First of all, in areas without samples (northwest and southeast corners of the site), we have no confidence in being able to find or not find hot spots. Even in areas with samples, we only have confidence in being able to find hot spots of dimensions greater than or equal to the spacing of the samples. Furthermore, it should be verified whether the entire area presented in Fig. 4c is needed for the evaluation. Specifically, if there are any portions of the site that the child recreator may not be able to access (e.g., due to fencing or other barriers), these areas are not part of the exposure area for the potential receptor and should be removed from the delineation. Lastly, even if the algorithm does not lead conclusively to hot spot delineation, it may provide guidance in directing the collection of additional samples. In particular, sampling within and/or around the delineated area may be used to refine and confirm the delineation, and collection of additional samples in areas with low sample density would increase confidence that undetected hot spots do not exist.

In summary, some important considerations relate to the application of the hot spot algorithm to environmental data sets. For a given sample density, the hot spot algorithm performs better for larger hot spots (relative to the total site area), since the likelihood of randomly sampling within the hot spot increases for larger hot spots. The boundaries of the total site area are not arbitrary, but are defined by the exposure area appropriate to a potential receptor. Confidence in hot spot delineation is largely dictated by sample density. For hot spots of diameter less than the spacing of samples, there is low confidence in being able to detect and delineate the hot spot. Collection of additional samples in areas with low sample density and within delineated areas will improve confidence in the hot spot delineation.

## 5. Conclusions

A risk-based approach to hot spot delineation was evaluated using Monte Carlo simulations. Random samples taken from a virtual site (“true site”) were used to create an interpolated site. The latter was gridded and concentrations from the center of each grid box were used to calculate 95% upper confidence limits on the mean site contaminant concentration and corresponding hazard quotients for a potential receptor. Grid cells with the highest concentrations were removed and hazard quotients were recalculated until the site hazard quotient dropped below the threshold of 1. The grid cells removed in this way define the spatial extent of the hot spot.

This hot spot delineation algorithm was applied to a Monte Carlo simulation of 100,000 iterations for the same true site, allowing the number and locations of samples to vary randomly. On average, the algorithm was able to delineate hot spots which were collocated with and equal to or greater in size than the “true hot spot.” When delineated hot spots were mapped onto the true site, setting contaminant concentrations in the mapped area to zero, the hazard quotients for these “remediated true sites” were

calculated. On average, these hazard quotients were within 5% of the acceptable threshold of 1.

### Acknowledgements

We are grateful to Dylan Small, Christopher Voci, and Swiatoslaw Kaczmar for their internal review of this paper. We thank the anonymous peer reviewers for their insightful comments which helped improve this paper. We are grateful to O'Brien and Gere for their encouragement of original technical research.

### References

- [1] N. Cressie, *Statistics for Spatial Data*, Wiley, New York, NY, 1991.
- [2] M. Kulldorff, A spatial scan statistic, *Commun. Statist.: Theory Methods* 26 (1997) 1481–1496.
- [3] G.P. Patil, C. Taillie, Use of best linear unbiased prediction for hot spot identification in two-way compositing, *Environ. Ecol. Statist.* 8 (2001) 163–169.
- [4] J.H. Carson Jr., Analysis of composite sampling data using the principle of maximum entropy, *Environ. Ecol. Statist.* 8 (2001) 201–211.
- [5] Oregon Department of Environmental Quality (ODEQ), *Guidance for Identification of Hot Spots*, Waste Management and Cleanup Division, Portland, OR, 1998.
- [6] R.N. Stewart, SADA: freeware for initial sample designs for environmental assessment, in: *Society for Risk Analysis Conference*, Baltimore, MD, 2003.
- [7] D.T. Sandwell, Biharmonic Spline Interpolation of GEOS-3 and SEASAT Altimeter Data, *Geophys. Res. Lett.* 2 (1987) 139–142.
- [8] United States Environmental Protection Agency (USEPA), *Risk Assessment Guidance for Superfund, vol. I: Human Health Evaluation Manual (Part A), Interim Final*, EPA/540/1-89/002, Office of Emergency and Remedial Response, Washington, DC, 1989.
- [9] USEPA, *Exposure Factors Handbook*, EPA/600/P-95/002F, Office of Research and Development, Washington, DC, 1997.
- [10] USEPA, *Integrated Risk Information System, Substance File for Antimony, Oral RfD Assessment, 1991* (available at: <http://www.epa.gov/IRIS/subst/0006.htm>).
- [11] R.O. Gilbert, *Statistical Methods for Environmental Pollution Monitoring*, Wiley, New York, NY, 1987.